The Astrophysical Journal Letters, 795:L32 (5pp), 2014 November 10 doi:10.1088/2041-8205/795/2/L32

PLASMA EMISSION BY WEAK TURBULENCE PROCESSES

L. F. Ziebell[1], P. H. Yoon[2,3], R. Gaelzer[1], and J. Pavan[4]
[1] Instituto de Física, UFRGS, Porto Alegre, RS, Brazil; luiz.ziebell@ufrgs.br, rudi.gaelzer@ufrgs.br
[2] Institute for Physical Science & Technology, University of Maryland, College Park, MD, USA; yoonp@umd.edu
[3] School of Space Research, Kyung Hee University, Yongin, Korea
[4] Instituto de Física e Matemática, UFPel, Pelotas, RS, Brazil; joel.pavan@ufpel.edu.br
Received 2014 September 29; accepted 2014 October 8; published 2014 October 27

ABSTRACT

The plasma emission is the radiation mechanism responsible for solar type II and type III radio bursts. The first theory of plasma emission was put forth in the 1950s, but the rigorous demonstration of the process based upon first principles had been lacking. The present Letter reports the first complete numerical solution of electromagnetic weak turbulence equations. It is shown that the fundamental emission is dominant and unless the beam speed is substantially higher than the electron thermal speed, the harmonic emission is not likely to be generated. The present findings may be useful for validating reduced models and for interpreting particle-in-cell simulations.

Key words: radiation mechanisms: non-thermal – solar wind – Sun: radio radiation – turbulence

Online-only material: color figures

1. INTRODUCTION

Partial conversion of electrostatic wave energy to transverse electromagnetic (EM) wave energy during the late nonlinear stage of the bump-on-tail instability is called the plasma emission process, and the resultant radiation emission occurs at the plasma frequency and/or its harmonic(s). It is believed that the plasma emission is responsible for the solar type II and type III radio bursts (McLean & Labrum 1985; Goldman 1983; Melrose 1986). According to the standard theoretical paradigm, based upon the first theory proposed in the 1950s (Ginzburg & Zheleznyakov 1958), an electron beam interacting with the background plasma excites Langmuir (L) waves via the bump-on-tail instability, followed by nonlinear processes of wave decay and scattering, eventually leading to the generation of EM radiation.

Such an elaborate process can, in principle, be demonstrated on the basis of EM weak turbulence theory—the fundamental equations thereof and their derivation can be found, e.g., in (Yoon 2006; Yoon et al. 2012; Ziebell et al. 2014b). Indeed, over the past several decades, the physics of plasma emission was discussed within the framework of reduced or partial EM weak turbulence theory (McLean & Labrum 1985; Goldman 1983; Melrose 1986; Robinson & Cairns 1998a, 1998b, 1998c; Li et al. 2008a, 2008b, 2009). However, the complete numerical solution of the entire set of EM weak turbulence equations has not been done hitherto. Instead, various approximations and simplifications have been made, which include the assumption of saturated wave amplitudes, predetermination of certain nonlinear processes being the most important, reduction of the equations to one-dimensional (1D) models, etc.

The above comments are not meant to diminish the value of reduced theories, however, as some of these theories, especially those of Li et al. (2008a, 2008b, 2009) and Schmidt & Cairns (2014), have advanced to the point where simple, yet reliable, plasma emission models are incorporated into macroscopic models so as to yield global-kinetic models with predictive capabilities. Nevertheless, since reduced models are based upon various assumptions, it is difficult to quantify the validity of such approaches unless there exists a benchmark full numerical solution. The present Letter reports the first ever complete numerical solutions of the EM weak turbulence equations in the presence of a beam, and the ensuing plasma emission. On the basis of the present results, detailed verification of various approximate theories can be done, but such a task is not the immediate focus of the present work.

One of the outstanding problems in the theory of plasma emission is whether the radiation is at the plasma frequency (fundamental emission) or at the first harmonic of the plasma frequency (harmonic emission). Reduced theories cannot determine the relative importance of the two emission bands.

Before we proceed, it should be mentioned that a handful of authors carried out direct EM particle-in-cell (PIC) simulations in order to characterize the nonlinear behavior of the plasma emission process (Kasaba et al. 2001; Rhee et al. 2009a, 2009b). The present full solution of EM weak turbulence equations is complementary to PIC simulation efforts.

2. THEORETICAL FORMULATION

The wave intensities for plasma normal modes are defined by their electric field energy. For longitudinal modes, the intensities $I_{\mathbf{k}}^{\sigma\alpha}$ for $\alpha = L, S$, where L and S stand for Langmuir and ion sound, respectively, are defined by

$$\langle \delta E_{\parallel}^2 \rangle_{\mathbf{k},\omega} = \sum_{\sigma=\pm1} \sum_{\alpha=L,S} I_{\mathbf{k}}^{\sigma\alpha} \delta\big(\omega - \sigma\omega_{\mathbf{k}}^{\alpha}\big).$$

The transverse mode T has both electric and magnetic fields, but it is sufficient to define the spectral wave intensity in terms of electric field,

$$\langle \delta E_{\perp}^2 \rangle_{\mathbf{k}\omega} = \sum_{\sigma=\pm1} I_{\mathbf{k}}^{\sigma T}\ \delta\big(\omega - \sigma\omega_{\mathbf{k}}^{T}\big),$$

as the magnetic field intensity is trivially given by $\langle \delta B^2 \rangle_{\mathbf{k}\omega} = |ck/\omega|^2 \langle \delta E_{\perp}^2 \rangle_{\mathbf{k}\omega}$. The linear dispersion relations for electrostatic (Langmuir L and ion-sound S) and transverse EM (T) modes are given by

$$\begin{aligned}
\omega_{\mathbf{k}}^{L} &= \omega_{pe}\left(1 + 3k^2\lambda_D^2/2\right),\\
\omega_{\mathbf{k}}^{S} &= kc_S\,(1 + 3T_e/T_i)^{1/2}\left(1 + k^2\lambda_D^2\right)^{-1/2},\\
\omega_{\mathbf{k}}^{T} &= \left(\omega_{pe}^2 + c^2k^2\right)^{1/2},
\end{aligned}$$

where $\omega_{\rm pe} = (4\pi n_e e^2/m_e)^{1/2}$ is the plasma frequency, n_e, e, and m_e being the electron number density, unit electric charge, and electron mass, respectively, $\lambda_D = [T_e/(4\pi n_e e^2)]^{1/2}$ is the Debye length, T_e and T_i are electron and ion temperatures, respectively, and $c_S = (T_e/m_i)^{1/2}$ represents the ion-sound speed, m_i being the ion (proton) mass. The L mode wave kinetic equation is given by

$$\begin{aligned}
\frac{\partial I_{\mathbf{k}}^{\sigma L}}{\partial t} &= \frac{4\pi e^2}{m_e k^2}\int d\mathbf{v}\,\delta\big(\sigma\omega_{\mathbf{k}}^L - \mathbf{k}\cdot\mathbf{v}\big) \\
&\quad\times\left(n_e e^2 F_e(\mathbf{v}) + \pi\sigma\omega_{\mathbf{k}}^L \mathbf{k}\cdot\frac{\partial F_e(\mathbf{v})}{\partial\mathbf{v}} I_{\mathbf{k}}^{\sigma L}\right) \\
&\quad+\sum_{\sigma',\sigma''=\pm 1}\int d\mathbf{k}'\,V_{\mathbf{k},\mathbf{k}'}^L\left(\frac{\sigma\omega_{\mathbf{k}}^L I_{\mathbf{k}'}^{\sigma' L} I_{\mathbf{k}-\mathbf{k}'}^{\sigma'' S}}{\mu_{\mathbf{k}-\mathbf{k}'}} - \frac{\sigma'\omega_{\mathbf{k}'}^L I_{\mathbf{k}-\mathbf{k}'}^{\sigma'' S} I_{\mathbf{k}}^{\sigma L}}{\mu_{\mathbf{k}-\mathbf{k}'}}\right. \\
&\quad\left. - \sigma''\omega_{\mathbf{k}-\mathbf{k}'}^L I_{\mathbf{k}'}^{\sigma' L} I_{\mathbf{k}}^{\sigma L}\right)\delta\big(\sigma\omega_{\mathbf{k}}^L - \sigma'\omega_{\mathbf{k}'}^L - \sigma''\omega_{\mathbf{k}-\mathbf{k}'}^S\big) \\
&\quad+\sum_{\sigma'}\int d\mathbf{k}'\int d\mathbf{v}\,U_{\mathbf{k},\mathbf{k}'}^L\,\delta\big[\sigma\omega_{\mathbf{k}}^L - \sigma'\omega_{\mathbf{k}'}^L - (\mathbf{k}-\mathbf{k}')\cdot\mathbf{v}\big] \\
&\quad\times\left[\frac{n_e e^2}{\omega_{\rm pe}^2}\big(\sigma\omega_{\mathbf{k}}^L I_{\mathbf{k}'}^{\sigma' L}[F_e(\mathbf{v}) + F_i(\mathbf{v})] - \sigma'\omega_{\mathbf{k}'}^L I_{\mathbf{k}}^{\sigma L}\big)\right. \\
&\quad\left.+\frac{\pi m_e}{m_i} I_{\mathbf{k}'}^{\sigma' L} I_{\mathbf{k}}^{\sigma L}(\mathbf{k}-\mathbf{k}')\cdot\frac{\partial F_i(\mathbf{v})}{\partial\mathbf{v}}\right], \qquad (1)
\end{aligned}$$

where

$$\begin{aligned}
V_{\mathbf{k},\mathbf{k}'}^L &= \frac{\pi e^2\sigma\omega_{\mathbf{k}}^L}{2T_e^2}\frac{\mu_{\mathbf{k}-\mathbf{k}'}(\mathbf{k}\cdot\mathbf{k}')^2}{k^2 k'^2|\mathbf{k}-\mathbf{k}'|^2}, \\
U_{\mathbf{k},\mathbf{k}'}^L &= \frac{\sigma\omega_{\mathbf{k}}^L e^2}{n_e m_e^2\omega_{\rm pe}^2}\frac{(\mathbf{k}\cdot\mathbf{k}')^2}{k^2 k'^2}, \\
\mu_{\mathbf{k}} &= |k|^3\lambda_D^3\left(\frac{m_e}{m_i}\right)^{1/2}\left(1+\frac{3T_i}{T_e}\right)^{1/2}. \qquad (2)
\end{aligned}$$

The first velocity integral term on the right-hand side of Equation (1) that contains the resonance factor $\delta(\sigma\omega_{\mathbf{k}}^L - \mathbf{k}\cdot\mathbf{v})$ (i.e., linear wave-particle interaction) represents the spontaneous and induced emissions of L waves, which are essentially quasilinear processes; the second $\mathbf{k}'$-integral term dictated by the three-wave resonance condition $\delta(\sigma\omega_{\mathbf{k}}^L - \sigma'\omega_{\mathbf{k}'}^L - \sigma''\omega_{\mathbf{k}-\mathbf{k}'}^S)$ (nonlinear three-wave interaction) represents the decay/coalescence involving L mode with another L mode and an S mode; the double integral term $\int d\mathbf{v}\int d\mathbf{k}'\cdots$ dictated by the nonlinear wave-particle resonance condition $\delta[\sigma\omega_{\mathbf{k}}^L - \sigma'\omega_{\mathbf{k}'}^L - (\mathbf{k}-\mathbf{k}')\cdot\mathbf{v}]$ represents the spontaneous and induced scattering processes involving two Langmuir waves and the particles.

For the ion-sound mode, $\alpha = S$, the wave kinetic equation is given by

$$\begin{aligned}
\frac{\partial}{\partial t}\frac{I_{\mathbf{k}}^{\sigma S}}{\mu_{\mathbf{k}}} &= \frac{4\pi\mu_{\mathbf{k}} e^2}{m_e k^2}\int d\mathbf{v}\,\delta\big(\sigma\omega_{\mathbf{k}}^S - \mathbf{k}\cdot\mathbf{v}\big)\Big[n_e e^2[f_e(\mathbf{v}) + f_i(\mathbf{v})] \\
&\quad+\pi\sigma\omega_{\mathbf{k}}^L\left(\mathbf{k}\cdot\frac{\partial f_e(\mathbf{v})}{\partial\mathbf{v}} + \frac{m_e}{m_i}\mathbf{k}\cdot\frac{\partial f_i(\mathbf{v})}{\partial\mathbf{v}}\right)\frac{I_{\mathbf{k}}^{\sigma S}}{\mu_{\mathbf{k}}}\Big] \\
&\quad+\sum_{\sigma',\sigma''}\int d\mathbf{k}'\,V_{\mathbf{k},\mathbf{k}'}^S\left(\sigma\omega_{\mathbf{k}}^L I_{\mathbf{k}'}^{\sigma' L} I_{\mathbf{k}-\mathbf{k}'}^{\sigma'' L} - \frac{\sigma'\omega_{\mathbf{k}'}^L I_{\mathbf{k}-\mathbf{k}'}^{\sigma'' L} I_{\mathbf{k}}^{\sigma S}}{\mu_{\mathbf{k}}}\right. \\
&\quad\left.-\frac{\sigma''\omega_{\mathbf{k}-\mathbf{k}'}^L I_{\mathbf{k}'}^{\sigma' L} I_{\mathbf{k}}^{\sigma S}}{\mu_{\mathbf{k}}}\right)\delta\big(\sigma\omega_{\mathbf{k}}^S - \sigma'\omega_{\mathbf{k}'}^L - \sigma''\omega_{\mathbf{k}-\mathbf{k}'}^L\big), \qquad (3)
\end{aligned}$$

where

$$V_{\mathbf{k},\mathbf{k}'}^S = \frac{\pi e^2\sigma\omega_{\mathbf{k}}^L}{4T_e^2}\frac{\mu_{\mathbf{k}}[\mathbf{k}'\cdot(\mathbf{k}-\mathbf{k}')]^2}{k^2 k'^2|\mathbf{k}-\mathbf{k}'|^2}. \qquad (4)$$

The first velocity integral term on the right-hand side of Equation (3) that contains the resonance factor $\delta(\sigma\omega_{\mathbf{k}}^S - \mathbf{k}\cdot\mathbf{v})$ represents the spontaneous and induced emissions of S waves. The $\mathbf{k}'$-integral term dictated by the three-wave resonance condition $\delta(\sigma\omega_{\mathbf{k}}^S - \sigma'\omega_{\mathbf{k}'}^L - \sigma''\omega_{\mathbf{k}-\mathbf{k}'}^S)$ corresponds to the decay/coalescence involving S mode with two L modes.

For the transverse mode T, the wave kinetic equation is given by

$$\begin{aligned}
\frac{\partial}{\partial t}\frac{I_{\mathbf{k}}^{\sigma T}}{2} &= \sum_{\sigma',\sigma''}\int d\mathbf{k}'\,V_{\mathbf{k},\mathbf{k}'}^{TLL}\left(\sigma\omega_{\mathbf{k}}^T I_{\mathbf{k}'}^{\sigma' L} I_{\mathbf{k}-\mathbf{k}'}^{\sigma'' L} - \frac{\sigma'\omega_{\mathbf{k}'}^L I_{\mathbf{k}-\mathbf{k}'}^{\sigma'' L} I_{\mathbf{k}}^{\sigma T}}{2}\right. \\
&\quad\left.-\frac{\sigma''\omega_{\mathbf{k}-\mathbf{k}'}^L I_{\mathbf{k}'}^{\sigma' L} I_{\mathbf{k}}^{\sigma T}}{2}\right)\delta\big(\sigma\omega_{\mathbf{k}}^T - \sigma'\omega_{\mathbf{k}'}^L - \sigma''\omega_{\mathbf{k}-\mathbf{k}'}^L\big) \\
&\quad+\sum_{\sigma',\sigma''}\int d\mathbf{k}'\,V_{\mathbf{k},\mathbf{k}'}^{TLS}\left(\frac{\sigma\omega_{\mathbf{k}}^T I_{\mathbf{k}'}^{\sigma' L} I_{\mathbf{k}-\mathbf{k}'}^{\sigma'' S}}{\mu_{\mathbf{k}-\mathbf{k}'}}\right. \\
&\quad\left.-\frac{\sigma'\omega_{\mathbf{k}'}^L I_{\mathbf{k}-\mathbf{k}'}^{\sigma'' S} I_{\mathbf{k}}^{\sigma T}}{2\mu_{\mathbf{k}-\mathbf{k}'}^S} - \frac{\sigma''\omega_{\mathbf{k}-\mathbf{k}'}^L I_{\mathbf{k}'}^{\sigma' L} I_{\mathbf{k}}^{\sigma T}}{2}\right) \\
&\quad\times\delta\big(\sigma\omega_{\mathbf{k}}^T - \sigma'\omega_{\mathbf{k}'}^L - \sigma''\omega_{\mathbf{k}-\mathbf{k}'}^S\big) \\
&\quad+\sum_{\sigma',\sigma''}\int d\mathbf{k}'\,V_{\mathbf{k},\mathbf{k}'}^{TTL}\left(\frac{\sigma\omega_{\mathbf{k}}^T I_{\mathbf{k}'}^{\sigma' T} I_{\mathbf{k}-\mathbf{k}'}^{\sigma'' L}}{2}\right. \\
&\quad\left.-\frac{\sigma'\omega_{\mathbf{k}'}^T I_{\mathbf{k}-\mathbf{k}'}^{\sigma'' L} I_{\mathbf{k}}^{\sigma T}}{2} - \frac{\sigma''\omega_{\mathbf{k}-\mathbf{k}'}^L I_{\mathbf{k}'}^{\sigma' T} I_{\mathbf{k}}^{\sigma T}}{4}\right) \\
&\quad\times\delta\big(\sigma\omega_{\mathbf{k}}^T - \sigma'\omega_{\mathbf{k}'}^T - \sigma''\omega_{\mathbf{k}-\mathbf{k}'}^L\big) \\
&\quad+\sum_{\sigma'}\int d\mathbf{k}'\int d\mathbf{v}\,U_{\mathbf{k},\mathbf{k}'}^T \\
&\quad\times\delta\big[\sigma\omega_{\mathbf{k}}^T - \sigma'\omega_{\mathbf{k}'}^L - (\mathbf{k}-\mathbf{k}')\cdot\mathbf{v}\big] \\
&\quad\times\left[\frac{n_e e^2}{\omega_{\rm pe}^2}\left(\sigma\omega_{\mathbf{k}}^T I_{\mathbf{k}'}^{\sigma' L} - \sigma'\omega_{\mathbf{k}'}^L\frac{I_{\mathbf{k}}^{\sigma T}}{2}\right)[F_e(\mathbf{v}) + F_i(\mathbf{v})]\right. \\
&\quad\left.+\pi\frac{m_e}{m_i} I_{\mathbf{k}'}^{\sigma' L}\frac{I_{\mathbf{k}}^{\sigma T}}{2}(\mathbf{k}-\mathbf{k}')\cdot\frac{\partial F_i(\mathbf{v})}{\partial\mathbf{v}}\right], \qquad (5)
\end{aligned}$$

where the elements of the interaction matrix are

$$\begin{aligned}
V_{\mathbf{k},\mathbf{k}'}^{TLL} &= \frac{\pi e^2\sigma\omega_{\mathbf{k}}^T}{32 m_e^2\omega_{\rm pe}^2}\frac{(\mathbf{k}\times\mathbf{k}')^2}{k^2 k'^2|\mathbf{k}-\mathbf{k}'|^2}\left(\frac{k'^2}{\sigma'\omega_{\mathbf{k}'}^L} - \frac{|\mathbf{k}-\mathbf{k}'|^2}{\sigma''\omega_{\mathbf{k}-\mathbf{k}'}^L}\right)^2, \\
V_{\mathbf{k},\mathbf{k}'}^{TLS} &= \frac{\pi e^2\sigma\omega_{\mathbf{k}}^T}{4T_e^2}\frac{\mu_{\mathbf{k}-\mathbf{k}'}(\mathbf{k}\times\mathbf{k}')^2}{k^2 k'^2|\mathbf{k}-\mathbf{k}'|^2}, \\
V_{\mathbf{k},\mathbf{k}'}^{TTL} &= \frac{\pi e^2\sigma\omega_{\mathbf{k}}^T}{4m_e^2}\frac{|\mathbf{k}-\mathbf{k}'|^2}{\big(\omega_{\mathbf{k}}^T\big)^2\big(\omega_{\mathbf{k}'}^T\big)^2}\left(1+\frac{(\mathbf{k}\cdot\mathbf{k}')^2}{k^2 k'^2}\right), \\
U_{\mathbf{k},\mathbf{k}'}^T &= \frac{\sigma\omega_{\mathbf{k}}^T e^2}{2n_e m_e^2\omega_{\rm pe}^2}\frac{(\mathbf{k}\times\mathbf{k}')^2}{k^2 k'^2}. \qquad (6)
\end{aligned}$$

The first $\mathbf{k}'$-integral terms in Equation (5) dictated by the three-wave resonance condition $\delta(\sigma\omega_{\mathbf{k}}^T - \sigma'\omega_{\mathbf{k}'}^L - \sigma''\omega_{\mathbf{k}-\mathbf{k}'}^L)$ represents the coalescence of two L modes into a T mode at the second harmonic plasma frequency. This process is responsible for the harmonic emission ($T \leftrightarrow L+L$). The next $\mathbf{k}'$ integrals associated with the factor $\delta(\sigma\omega_{\mathbf{k}}^T - \sigma'\omega_{\mathbf{k}'}^L - \sigma''\omega_{\mathbf{k}-\mathbf{k}'}^S)$

describe the merging of L and S modes into a T mode at the fundamental plasma frequency. This is one of the processes responsible for the fundamental emission ($T \leftrightarrow L + S$). The third $\mathbf{k}'$ integrals with $\delta(\sigma\omega^T_{\mathbf{k}} - \sigma'\omega^T_{\mathbf{k}'} - \sigma''\omega^L_{\mathbf{k}-\mathbf{k}'})$ depict the merging of a T mode and an L mode into the next higher harmonic T mode. This process, known as the incoherent Raman scattering, is responsible for generating higher-harmonic plasma emission ($T \leftrightarrow T + L$). The double integral term $\int d\mathbf{v} \int d\mathbf{k}' \cdots$ dictated by the nonlinear wave-particle resonance condition $\delta[\sigma\omega^T_{\mathbf{k}} - \sigma'\omega^L_{\mathbf{k}'} - (\mathbf{k}-\mathbf{k}')\cdot\mathbf{v}]$ represents spontaneous and induced scattering processes involving T and L modes and the particles, largely dominated by thermal protons ($T \leftrightarrow p + L$), but also electrons ($T \leftrightarrow e + L$). This process represents an alternative mechanism for the fundamental emission.

Finally, the formal particle kinetic equation is given by

$$\frac{\partial F_a(\mathbf{v})}{\partial t} = \frac{\pi e_a^2}{m_a^2} \sum_{\sigma=\pm1} \sum_{\alpha=L,S} \int d\mathbf{k} \frac{\mathbf{k}}{k} \cdot \frac{\partial}{\partial \mathbf{v}} \delta\left(\sigma\omega^\alpha_{\mathbf{k}} - \mathbf{k}\cdot\mathbf{v}\right) \times \left(\frac{m_a \mu^\alpha_{\mathbf{k}} \sigma \omega^L_{\mathbf{k}}}{4\pi^2 k} F_a(\mathbf{v}) + I^{\sigma\alpha}_{\mathbf{k}} \frac{\mathbf{k}}{k} \cdot \frac{\partial F_a(\mathbf{v})}{\partial \mathbf{v}} \right), \tag{7}$$

where $a = i, e$ stands for ions and electrons, respectively, and $\mu^L_{\mathbf{k}} = 1$ and $\mu^S_{\mathbf{k}} = \mu_{\mathbf{k}}$.

3. NUMERICAL ANALYSIS

We developed a sophisticated numerical routine termed the EM weak turbulence simulation code to solve the complete set of Equations (1)–(7) in a self-consistent manner. It adopts the normalized time, $\omega_{\mathrm{pe}}t$, dimensionless wave frequency and wave vector, $\omega/\omega_{\mathrm{pe}}$ and $\mathbf{k}v_{\mathrm{th}}/\omega_{\mathrm{pe}}$, where v_{th} corresponds to the thermal speed associated with the background electrons, and dimensionless velocity vector, $\mathbf{v}/v_{\mathrm{th}}$. The spectral wave intensity is defined by

$$\frac{(2\pi)^2 g}{m_e v_{\mathrm{th}}^2} \frac{I^{\sigma\alpha}_{\mathbf{k}}}{\mu^\alpha_{\mathbf{k}}}, \tag{8}$$

where $\mu^L_{\mathbf{k}} = 1$, $\mu^S_{\mathbf{k}} = \mu_{\mathbf{k}}$, as noted before, $\mu^T_{\mathbf{k}} = 1$, and $g = 1/[2^{3/2}(4\pi)^2 n_e \lambda_D^3]$ is related to the customary plasma parameter, $1/(n_e\lambda_D^3)$, which is taken to be 5×10^{-3}. Of course, in the actual heliospheric environment, this number should be much smaller, on the order of 10^{-8} or so, but we adopted an unrealistically high value of the plasma parameter in order to facilitate the numerical procedure, since a realistically small number would bring the initial wave level to a tiny value, delaying the linear growth, and therefore the overall evolution.

We solved the complete set of equations for initial configuration in which the ions are considered stationary and distributed according to the thermal equilibrium model with temperature T_i, and the electrons are composed of an isotropic thermal background plus a Gaussian distribution of a streaming component. The initial drift speed of the beam is denoted by V_b, and the temperature of the background electrons are designated by T_e. The ratio of the beam electron density n_b and the background electron density n_0 is assumed to be $n_b/n_0 = 10^{-3}$, and the beam is assumed to propagate in the z direction. The Gaussian thermal spread associated with the beam is taken to be the same as that of the background electron thermal speed, and we assume that the ion-to-electron temperature ratio is $T_i/T_e = 1/7$. The discretized time step for numerical computation is chosen as $\Delta t = 0.1\omega_{\mathrm{pe}}^{-1}$, and we use two-dimensional (2D) velocity and wave number space, $-12 < (v_x/v_{\mathrm{th}}, v_z/v_{\mathrm{th}}) < 12$, where $v_{\mathrm{th}} = (2T/m_e)^{1/2}$ is the electron thermal speed, and $0 < (k_x v_{\mathrm{th}}/\omega_{\mathrm{pe}}, k_z v_{\mathrm{th}}/\omega_{\mathrm{pe}}) < 0.6$. We carried out a 2D numerical analysis since the plasma emission cannot take place in a 1D system. It should be noted that the present 2D approach captures all the necessary physics, and may be largely equivalent to a fully three-dimensional situation with a cylindrical symmetry. Finally, in the present EM weak turbulence theory, the ratio of electron thermal speed to the speed of light *in vacuo* must be prescribed. For the present purpose, we consider $v_{\mathrm{th}}^2/c^2 = 4.0 \times 10^{-3}$. In the low corona of the Sun, the typical electron thermal energy is $\sim 10^2$ eV; thus, the present choice is approximately equal to the coronal value.

In Figure 1, we showcase a typical numerical result. For this case, we considered the initial beam speed $V_b/v_{\mathrm{th}} = 6$, and have numerically integrated the complete equations up to the normalized time step $\omega_{\mathrm{pe}}t = 2 \times 10^3$. The description can be found in the figure caption. The electron distribution function shown in Figure 1(a) features a broad range of velocity-space plateau in the velocity space initially occupied by a beam, which is a result of quasilinear diffusion. The Langmuir turbulence spectrum in Figure 1(b) shows an enhanced forward-propagating component (the primary L), which is the result of initial bump-on-tail instability, and the backscattered component, which is the result of combined three-wave decay and nonlinear wave-particle interaction. Note that the morphology of the 2D L mode spectrum compares favorably with the simulated spectrum—see, e.g., Figure 2 of Rhee et al. (2009b). Nonlinear decay processes generate the ion-sound mode by decay instability, as indicated in Figure 1(c) by the "enhanced" and "weakly enhanced" range of 2D k space. Panel (d) of Figure 1 is the transverse EM mode spectrum. We plot the electric field intensity associated with the radiation, $I_T(\mathbf{k})$. The small k (or long wavelength) regime corresponds to the fundamental (F) emission near ω_{pe}, while the outer ring corresponds to the harmonic (H) emission with frequency in the vicinity of $2\omega_{\mathrm{pe}}$. In short, the present Letter reports the first ever theoretical demonstration of F/H pair emission starting from the beam-plasma instability, by allowing all the relevant nonlinear processes to operate. This is in contrast to other related works, e.g., (Li et al. 2008a, 2008b, 2009), where simplified approaches are taken at the outset. Our rigorous numerical solutions are comparable to the full PIC simulations (Kasaba et al. 2001; Rhee et al. 2009a, 2009b), and indeed we find that the comparison with simulation results is favorable. For instance, the present Figure 1(d) can be compared against the simulated radiation spectral pattern, e.g., Figures 3 and 4 of Rhee et al. (2009b). Upon visual inspection of the present Figure 1(d) and the simulated radiation pattern, it is quite obvious that the agreement is excellent. This shows that the present weak turbulence simulation is a reliable research tool for quantitative investigations of plasma emission phenomena, yet it is computationally much more efficient when compared with the full PIC code scheme.

We have repeated the self-consistent calculations for other parameters, but in Figure 2, we choose to show the angle-averaged electric field spectrum (in normalized form) versus the frequency $\omega/\omega_{\mathrm{pe}}$, for four different initial beam speeds, while other input parameters are held constant as in Figure 1. For $V_b/v_{\mathrm{th}} = 5$, Figure 2 shows that the F emission completely dominates over H emission, but as the normalized beam speed increases to $V_b/v_{\mathrm{th}} = 6$ we observe that the H component becomes more apparent. Proceeding to higher beam velocities, one can discern that the H component becomes progressively more intense, but it never becomes higher than the F component.

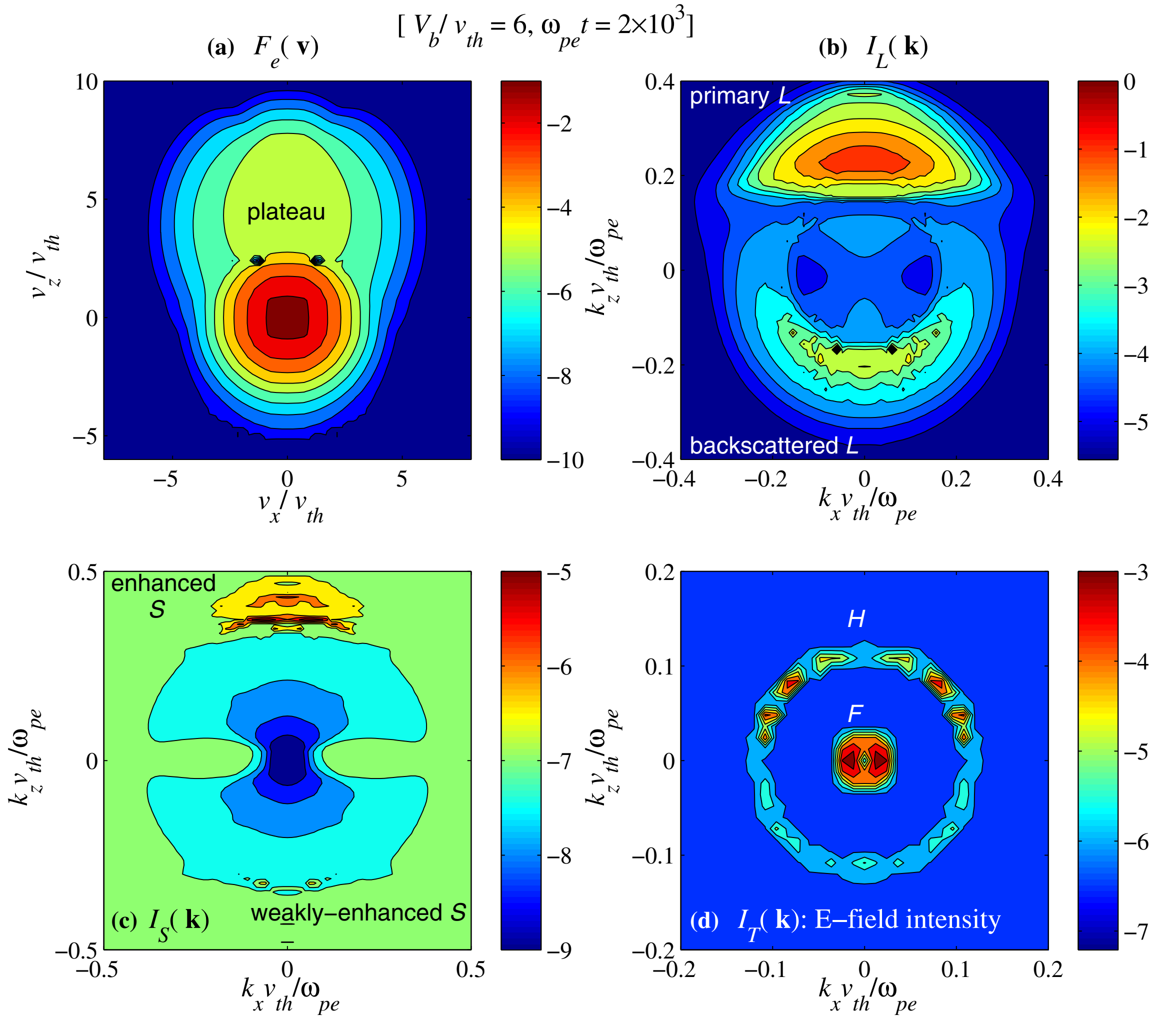

Figure 1. Panel (a) depicts the electron distribution function F_e vs. $v_x/v_{\rm th}$ and $v_z/v_{\rm th}$; panel (b) shows the Langmuir wave spectral intensity $I_L(\mathbf{k})$ vs. $k_x v_{\rm th}/\omega_{\rm pe}$ and $k_z v_{\rm th}/\omega_{\rm pe}$; panel (c) plots the wave spectral intensity corresponding to the ion-sound mode, $I_S(\mathbf{k})$; and panel (d) is the transverse mode electric field spectrum $I_T(\mathbf{k})$. The above results are at normalized time $\omega_{\rm pe}t = 2 \times 10^3$, with the initial condition $V_b/v_{\rm th} = 6$. Other input parameters are described in the text.

(A color version of this figure is available in the online journal.)

Note that for the case of $V_b/v_{\rm th} = 8$, there is a small, barely visible, enhancement at the third harmonic, $\omega \simeq 3\omega_{\rm pe}$. This is the result of the incoherent Raman process, $T \leftrightarrow T + L$, that generates higher harmonics. However, as one can see, the third-harmonic peak is extremely low so that, in general, higher harmonic plasma emission is not expected to be a common feature, which is consistent with observations. Also note that the transverse EM radiation at the plasma frequency and its harmonic takes place over a background level, as indicated in Figure 2. The theory of the background radiation for isotropic plasma in the absence of the beam was recently put forth by the present authors (Ziebell et al. 2014a), and it is supported by results obtained from PIC simulations (Ziebell et al. 2014b). It is this background level of radiation that partially hides the harmonic emission peak in the case of $V_b/v_{\rm th} = 5$. The theory of background radiation (Ziebell et al. 2014b) is based upon the nonlinear wave-particle interaction, which some reduced theories have ignored at the outset (Li et al. 2008a, 2008b, 2009). Judging from Figure 2(a), under certain conditions, one might obtain false H emission if one does not take the background radiation into account.

4. FINAL REMARKS

To summarize, despite many decades of theoretical research on the plasma emission, the actual numerical solution of the equations of EM weak turbulence theory that forms the basis of the plasma emission had not been available in the literature. In the absence of exact numerical solution, it is difficult to quantitatively verify the validity of various approximate models. The present Letter reports the first ever complete numerical solution of electromagnetic weak turbulence equations with which, the validity of various approximate theories (Li et al. 2008a, 2008b, 2009; Schmidt & Cairns 2014) can be tested, and it may also be employed to interpret the PIC simulations (Kasaba et al. 2001; Rhee et al. 2009a, 2009b). However, such a task is beyond the scope of the present work. One of the most interesting findings according to our complete numerical solutions is that the plasma emission must be dominated by the fundamental emission, and that the presence of harmonic emission may imply high average beam velocities. In fact, weak harmonic emission may be obscured by the background EM emission, which implies that if our numerical example is the

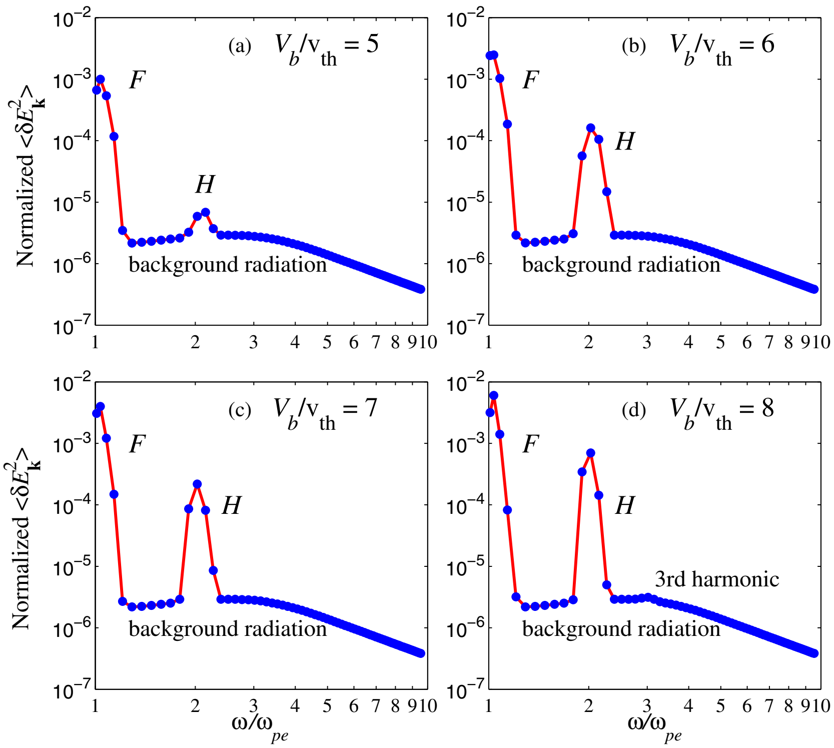

Figure 2. Panel (a) shows the normalized electric field intensity $\langle \delta E^2(\mathbf{k}) \rangle$ vs. normalized frequency $\omega/\omega_{\rm pe}$ for initial beam speed $V_b/v_{\rm th} = 5$; panel (b) corresponds to $V_b/v_{\rm th} = 6$; panel (c) corresponds to $V_b/v_{\rm th} = 7$; and panel (d) is the case of high beam speed, $V_b/v_{\rm th} = 8$. The above results are for normalized time $\omega_{\rm pe}t = 2 \times 10^3$. (A color version of this figure is available in the online journal.)

norm, then most of the plasma emission has to take place at the fundamental plasma frequency. We should caution that this conclusion is based upon the weak turbulence paradigm. Alternative models of plasma emission, e.g., one that is based upon the concept of strong turbulence (Robinson, 1997), are not the focus of the present Letter.

This work has been partially supported by the Brazilian agencies CNPq and FAPERGS. P.H.Y. acknowledges NSF grant AGS1242331 and the BK21 plus grant from the National Research Foundation (NRF) of the Republic of Korea.

REFERENCES

Ginzburg, C. L., & Zheleznyakov, V. V. 1958, SvA, 2, 653
Goldman, M. V. 1983, SoPh, 89, 403
Kasaba, Y., Matsumoto, H., & Omura, Y. 2001, JGR, 106, 18693
Li, B., Cairns, I. H., & Robinson, P. A. 2008a, JGR, 113, A06104
Li, B., Cairns, I. H., & Robinson, P. A. 2008b, JGR, 113, A06105
Li, B., Cairns, I. H., & Robinson, P. A. 2009, JGR, 114, A02104
McLean, D. L., & Labrum, N. R. (eds.) 1985, Solar Radiophysics (New York: Cambridge University Press)
Melrose, D. B. 1986, Instabilities in Space and Laboratory Plasmas (New York: Cambridge University Press)
Rhee, T., Ryu, C.-M., Woo, M., et al. 2009a, ApJ, 694, 618
Rhee, T., Woo, M., & Ryu, C.-M. 2009b, JKPS, 54, 313
Robinson, P. A. 1997, RvMP, 69, 507
Robinson, P. A., & Cairns, I. H. 1998a, SoPh, 181, 363
Robinson, P. A., & Cairns, I. H. 1998b, SoPh, 181, 395
Robinson, P. A., & Cairns, I. H. 1998c, SoPh, 181, 429
Schmidt, J. M., & Cairns, I. H. 2014, JGR, 119, 69
Yoon, P. H. 2006, PhPl, 13, 022302
Yoon, P. H., Ziebell, L. F., Gaelzer, R., & Pavan, J. 2012, PhPl, 19, 102303
Ziebell, L. F., Yoon, P. H., Gaelzer, R., & Pavan, J. 2014a, PhPl, 21, 012306
Ziebell, L. F., Yoon, P. H., Simões, F. J. R., Gaelzer, R., & Pavan, J. 2014b, PhPl, 21, 010701